Available online at www.jourcc.com

Journal homepage: www.JOURCC.com

Journal of Composites and Compounds

Poly (d/l) lactide-polycaprolactone/bioactive glass nanocomposites: assessments of in vitro bioactivity and biodegradability

Javad Esmaeilzadeh [a]*, *Saeed Hesaraki* [b], *Shokoufeh Borhan* [c]

[a] *Central Research Laboratory, Esfarayen University of Technology, Esfarayen, North Khorasan, Iran*

[b] *Biomaterials Group, Nanotechnology and Advanced Materials Department, Materials and Energy Research Center, Tehran, Iran*

[c] *Department of Materials and Chemical Engineering, Imam Khomeini International University- Buin Zahra Higher Education Center of Engineering and Technology, Qazvin, Iran*

A B S T R A C T

The in vitro assessments suggested the essential features for the bio screws applications. The effects of bioactive glass nanoparticles (BG) during in vitro studies of the poly (D/L) lactide (PDLLA)/polycaprolactone (PCL)/ BG nanocomposites (PPB) were assessed. The PDLLA/PCL (PP) blends were chosen as control groups. Apatite formations capabilities, weight and pH variations, alkaline phosphatase activity (ALP), and MTT assay were assigned during different immersion times up to 6 months. The XRD and SEM results revealed the superior apatite formation of PPB in simulated body fluids (SBF) compared to PP. The weight loss and pH variation results illustrated the highest values related to PP. Moreover, the MG-63 cells cultures determined the better cell viability of the PPB compared to the PP blends. Although, there are no statistically significant differences between the two groups. In addition, similar trends are shown for the ALP results where these amounts after 2 and 3 weeks incubation are considerable for PPB in comparison to PP. However, there are also no statistically significant differences between the two groups. Overall, the in vitro bioactivity and biodegradability confirmed that the PPB implants can be promised as a proper candidate for anterior cruciate ligament reconstruction screws.

Peer review under responsibility of JCC Research Group

A R T I C L E I N F O R M A T I O N

Article history:
Received 26 October 2021
Received in revised form 28 November 2021
Accepted 25 December 2021

Keywords:
In vitro test
PDLLA/PCL
Bioactive glass nanoparticles
Bioactivity and biodegradation

1. Introduction

Currently, metallic screws are the most commonly used ligament graft fixation devices in anterior cruciate ligament reconstruction (ACLR). Metallic screws provide solid fixations and are generally well tolerated by the body, although they can cause lacerations of the grafts while they are inserted [1].Their potential interferences with future surgeries such as ACLR revision [2] and interposition with any future magnetic resonance imaging (MRI) studies are some of their limitations [3]. Additionally, the carcinogenic potential and the possibility of corrosion manner of metallic screws prompted the surgeon to recommend their removal during a second surgery. To overcome such problems, polymeric screws especially biodegradable ones may be a superior alternative for metallic screws [4]. Biodegradable screws are able to be resorbed during the determined time after implantation into the body and degradation products will be disappeared via metabolic routes [5]. However, there are some concerns with the use of biodegradable screws including breakage during insertion and inflammatory reactions which may cause absorption of the adjacent tissues. Moreover, they are not able to promote the bone ingrowths and subsequently leave voids in the tissue once the screws have been fully degraded [6]. Other limitations of biodegradable screws with respect to metallic ones are their relatively low values of Young modulus (E) and strength [7]. In this regard applying a screw with a thick diameter may be ensured the required stability. Also, reinforcing the polymeric matrix of biodegradable screws by adding a rigid phase could provide adequate strength and stiffness for bioscrews. In our previous studies, it was reported that the mechanical properties of poly(d/l)lactide (PDLLA)/polycaprolactone (PCL) blends including tensile strength, tensile modulus, flexural strength, and flexural modulus [8] as well as creep and creep recovery [9] improved by adding the sol-gel derived bioactive glass nanoparticles (BGn) into the matrix. Applying BGn can also stimulate bone ingrowth and provide a reservoir of calcium and phosphate ions, thus may accelerate the new bone formations and preventing void formations after screws removal [10]. Moreover, adjacent bones could interact with screws and attach to the bioactive fillers of bioscrews while the polymeric matrix is simultaneously degraded [11].

With respect to biodegradable ACL screws, the tailoring of degradation manners is significant, so, a harmonic trend between mechanical

* *Corresponding author: Javad Esmaeilzadeh; E-mail: esmaeilzadehj@esfarayen.ac.ir*
https://doi.org/10.52547/jcc.3.4.1

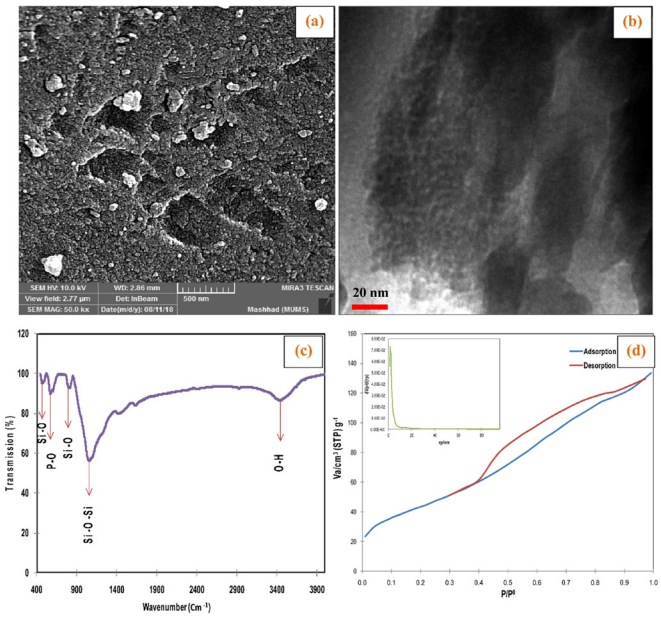

Fig. 1. Characterizations results of prepared BGn, (a) FESEM and (b) TEM micrographs, (c) FTIR spectrum analysis, and (d) BET and BJH measurements results.

properties and ligament healing process should be existed [12]. The *in vitro* evaluations have been extensively used to study biocompatibility and degradation behaviors of biodegradable implants [13-15]. These studies typically consist of evaluating implant degradation properties such as mass loss, pH variations, bone growth capabilities, and biomechanical behaviors in simulated body fluid (SBF) or phosphate-buffered saline (PBS).

There are many researchers who investigate the in vitro assessments of biodegradable polymeric materials and polymeric-based composites [19-20]. For example, *in-vitro* analysis in SBF solution for 1 week demonstrated that PLA/hydroxyapatite (HA) and PLA grafts have changed the pH, mass loss, morphology, and phase structure. This is due to the formation of the HA on the surface of the nanocomposites and the hydrolysis process of PLA after immersion in SBF solution [21]. Another research [22] reported the fabrication of synthetic bone graft substitutes composed of a polymer and a calcium-phosphate (Ca-P) ceramic. The *in-vitro* results showed that the weight loss for PLA/HA was greater than PLA particles upon 12-week immersion and PLA/HA strongly promotes the alkaline phosphatase (ALP) activity for mesenchymal stem cell (MSC) at osteogenic medium.

In the current work, PDLLA/PCL/BGn nanocomposites were developed using solvent casting manufacturing techniques. PLA as well-known linear aliphatic polyester with desirable mechanical properties and degradation capability in biotic and abiotic conditions allows use in ACLR screws. PCL is biodegradable semicrystalline polyester which due to its chain flexibility, can give a toughness feature to its blends when it blends with PLA matrix. *In-vitro* studies including mass loss, pH variations, and apatite formation capability were assessed. Besides, the human osteosarcoma cells (MG-63) were cultured on the nanocomposites and PDLLA/PCL as control, and cell proliferation and ALP activity

Table 1.
The blood plasma cations and anions compositions [24]

Cations	Concentration (× 10^{-3} M)	Anions	Concentration (× 10^{-3} M)
Na^{+}	142	Cl^{-}	148.8
K^{+}	5.0	HCO^{3-}	4.2
Mg^{2+}	1.5	HPO_4^{2-}	1.0
Ca^{2+}	2.5		

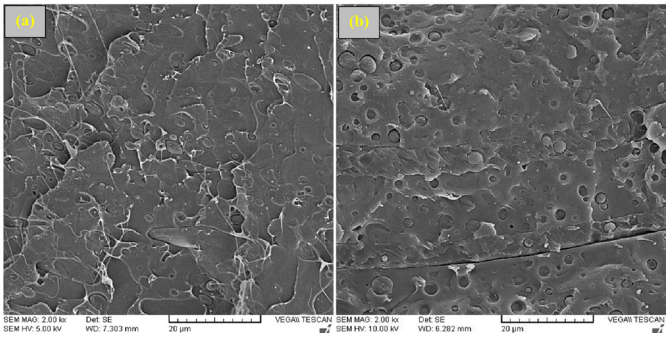

Fig. 2. SEM micrographs of the cryogenically fractured surface of the (a) neat PP and (b) PPB nanocomposites.

were also evaluated. It is hypothesized that the bioactive glass nanoparticles could enhance the bioactivity and biodegradation behaviors of PDLLA/PCL throughout the *in-vitro* assessments. According to the best of our knowledge, there are no or still few reports in the *in-vitro* studies of PDLLA/PCL/BGn triple nanocomposites for any bio-implants applications.

2. Materials and methods

2.1. Materials

The medical grade of PDLLA with CAS No. 26,023–30-3 used in the study purchased from Changchun Sinobiomaterials Co., Ltd (China). The ratio of L-LA to D-LA in PDLLA structure was 90:0, and it possess the inherent viscosity of 0.75–1.25 dl/g, average molecular weight of 56,000 g/mol and density of 1.2–1.3 g/ml. The medical-grade polycaprolactone (PCL) was purchased from Sigma Aldrich Co. The density and average molecular weight of it were 1.146 g/ml and 80,000 Da, respectively. The used BGn with chemical compositions of $64SiO_2$. $31CaO.5P_2O_5$ was also produced using the sol-gel procedure which is reported in our previous work [8].

2.2. Specimens preparation

The preparation details of PDLLA/PCL as control (PP) and PDLLA/PCL/BGn as nanocomposites (PPB) samples have been described in previous papers [8, 23]. Briefly, the control samples were produced by the introduction of the PCL phase into the PDLLA matrix phase in a portion of 20:80 dissolving in chloroform solvent. The nanocomposites samples were also prepared by adding 3 wt% BGn into PDLLA/PCL bipolymeric solution. After homogenization by stirring, the mixtures were cast and dried at 50 °C and 80 °C in an oven and vacuum oven, respectively to remove the solvent. Finally, the dried samples were poured into molds, compressed under 30 MPa at 180 °C followed by water-cooling to room temperature. Meanwhile, all samples were pressed under heating for less than 3 minutes.

2.3. In vitro degradation studies

In vitro degradation behaviors of controls and nanocomposites samples are performed in SBF solution as an acellular solution whose chemical composition is similar to that of blood plasma. The blood plasma composition is listed in Table 1 [24]. Samples were immersed into SBF at 37 °C at a pH of 7.4, keeping the ratio of the solution to the specimen 50:1 (ml:g) and followed for 8 weeks. The immersion solution was changed every 3 days up to 28 days. During the immersion time, each sample was studied in terms of phase, morphology, weight loss, and pH variations. Moreover, degradation behaviors of all samples in PBS were in a similar way compared with SBF. The compositions of PBS include sodium chloride, disodium hydrogen phosphate, and in some formula-

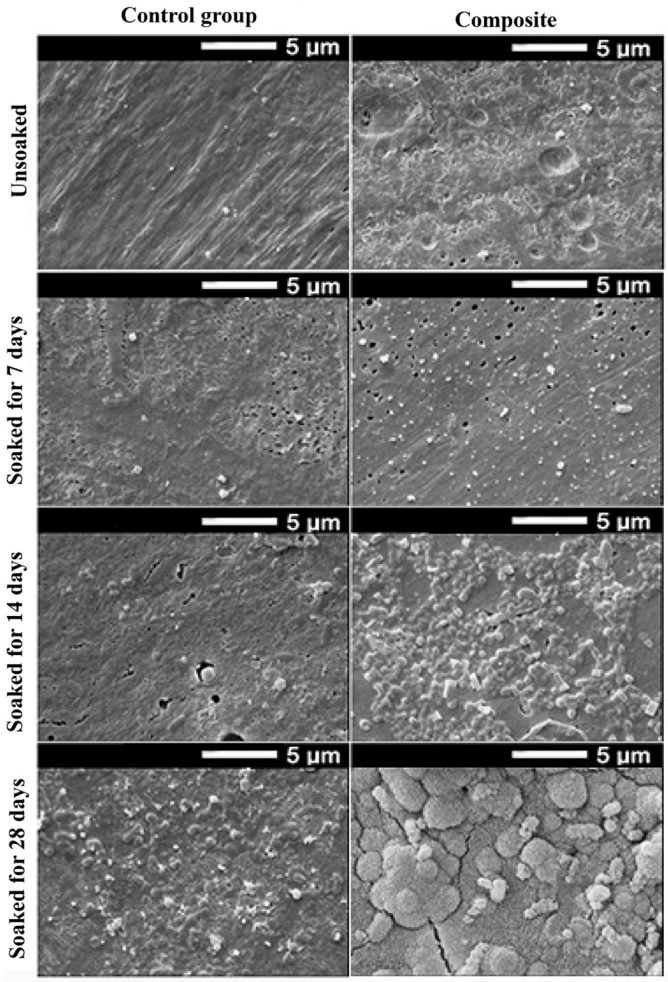

Fig. 3. SEM images of PPB nanocomposites and PP blends during different immersion times in SBF solutions.

tions contain potassium chloride and potassium dihydrogen phosphate which phosphate groups make pH of solution fix at 7.4.

2.3.1. Phase and morphological studies

Morphological analysis of the controls and nanocomposites surface, as well as phase variations, were carried out by scanning electron microscopy (SEM, Stereoscan S360 Cambridge) and X-ray diffraction (XRD, pw3710 Philips) analysis, respectively. For these reasons, the samples after soaking into SBF and PBS solutions at each following time period were removed from the solution, rinsed with deionized water, and dried at room temperature.

2.3.2. Weight loss variations and pH changes

The weight variations of controls and nanocomposites samples were studied at both SBF and PBS solutions. In this respect, all samples weights were measured using a balance with a sensitivity of 0.01 mg before and then after soaking for identified period times in biological solutions. In this procedure, the samples were taken from solutions, dried at room temperature for 24 hours, and were again weighted. The percentage of weight loss was estimated according to the following equation:

$$W_t\% = \frac{W_f - W_i}{W_i} \times 100$$

where, is the initial dry weight of the sample and is the dry weight of the sample at studying time periods. Values are expressed as the average of three replicates. Besides, the pH of solutions at each evaluating time period was measured. For *in-vitro* tests, the samples were chosen in disk shape with 3 and 8 mm in diameter and 1 mm in thickness.

2.4. Cell viability assays

2.4.1. Cell toxicity

To evaluate the cell adhesion and proliferation on control and nanocomposites cell behaviors, the human osteosarcoma (MG63) cell lines were prepared from the National Cell Bank of Iran (NCBI C 116). The derived cells were cultured in tissue culture polystyrene flasks (Falcon, USA) at 37 °C under 5% CO_2 atmosphere in Dulbecco's Modified Eagle's Medium (DMEM) with L-glutamine, supplemented with 10% fetal bovine serum (FBS) and antibiotic (100 units penicillin G sodium, 100 mg streptomycin sulfate, and 0.25 mg amphotericin B in saline) until the cell population into cultured flask reach to 70-80% density. After that, the cell lines were carefully washed with PBS solution followed harvested after the treatment with 0.05% trypsin–EDTA into an incubator medium for 3 minutes. The solution contains confluent cells that were centrifuged to separate. After removing the PBS solution, the FBS was added to cells, and cells were precisely pitajed to be utilized for the tests. The samples were disinfected using 70% ethanol and cells with a density of 1.2×10^4 cells per cm^2 were seeded on them. The specimen/cell constructs were then placed into 96-wells culture plates and kept undisturbed in an incubator at 37 °C in a humidified atmosphere of 95% air and 5% CO_2 for 24 h to allow the cells to adhere to the substrates. Finally, 300 µl culture medium was added into each well and then, the plates were put back into the incubator and left for 24, 72, and 168 hours. The medium was changed every 3 days. These tests were performed 3 times for each sample. At the end of each evaluating time period, the medium was taken out and 150 µl of 3-{4,5-dimethylthiazol-2yl}-2,5-diphenyl-2H-tetrazolium bromide (MTT) solution with a concentration of 0.5 µg/ml was added to each well. During each time period of studying, the plates were precisely covered by foil preventing light and incubated at 37 °C for 4 hours in the incubator. In fact, during these 4 hours, the succinate dehydrogenases as mitochondria enzymes give an opportunity to reduce into insoluble purple formazan granules. It should be noted that these formazan purple crystals have obviously been detected by optical microscopy. Subsequently, the medium was discarded and 350 µl dimethylsulfoxide (DMSO) was added to tetrazolium blue crystals converted to formazan purple crystals. Finally, the plate medium was transferred into other plates and the optical density of the solution was measured using a microplate spectrophotometer (BIO-TEK Elx 808, Highland Park, USA) at a wavelength of 570 nm.

2.4.2. Cell attachments

To observe the morphologies of the cells adhered to the surfaces of the specimens with dimensions of 5 mm in diameter and 1 mm in thickness, the cells were cultured on the specimens as described above. After 48 hours, the culture medium was removed, the cell-cultured specimens were rinsed with PBS twice and then the cells were fixed with 500 ml/well of 2.5% glutaraldehyde and 2% paraformaldehyde. After 30 min, they were again rinsed and kept in PBS at 4 °C. Specimens were then fixed with 1% Osmium tetroxide (Polyscience, Warmington, PA, USA). After cell fixation, the specimens were dehydrated in ethanol solutions of varying concentrations (50, 60, 70, 80, 90, and 100%) for about 10 minutes at each concentration. The specimens were then dried in the air, coated with gold, and analyzed by SEM.

2.4.3. Alkaline phosphatase (ALP) activity

The amount of level of alkaline phosphatase enzyme may be related to the osteoblast activity of samples. This enzyme could degrade the

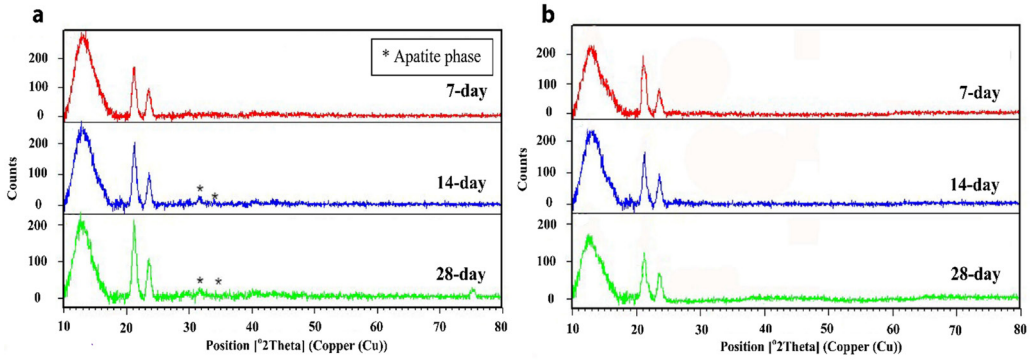

Fig. 4. XRD patterns of, (a) PPB nanocomposites and (b) PP blends immersed into SBF solutions for different time intervals of 1, 2, and 4 weeks.

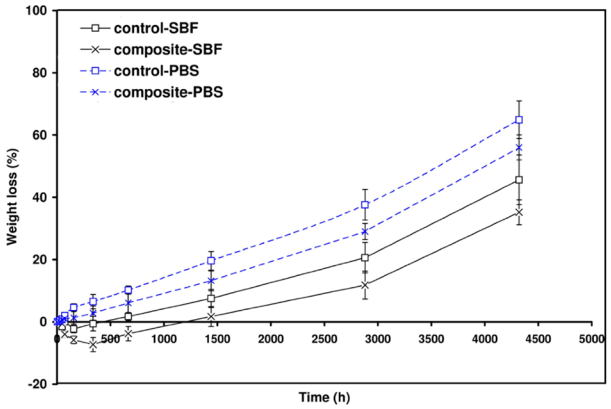

Fig. 5. Exhibitions of weight loss variations for PP and PPB specimens in SBF and PBS solutions during different immersion times up to 6 months.

inorganic pyrophosphate and provide a sufficient local concentration of phosphate and pyrophosphate which is crucial for the calcifying process of samples. For this purpose, the cells seeded on the samples under the same culturing condition as described above, the level of ALP was determined on days 3, 7, 14, and 21. ALP activity was determined at 405 nm using p-nitrophenyl phosphate in diethanol amide buffer as chromogenic substrate.

3. Results and discussions

3.1. Characterizations

The characterizations results of BGn bioactive phase are represented in Figure 1.

As can be seen in Figure 1a, the field emission SEM micrograph illustrates that the large particles of prepared BGn (with a size of about 1 μm) consist of many fine particles aggregated with each other which represented random-sized particles smaller than 50 nm. The TEM image of BGn (Figure 1b) shows a mesostructure composed exclusively of wormlike aggregates with acceptable interconnectivity morphology. In the BGn FTIR spectrum (Figure 1c), the wide and strong peak apeaered at 1063 cm^{-1} could be related to the stretch vibration of Si-O-Si groups. The bands at 809 and 478 cm^{-1} determin the typical symmetric stretch vibration of Si-O and the bending vibration of Si-O, respectively. The outspread peak observed at 570 cm^{-1} is ascribed to the bending vibration of amorphous P-O. Moreover, the peak that observed at 3450 cm^{-1} is indicative of the hydroxyl group at BGn surface. Figure 1d demonstrates the N_2 adsorption-desorption isotherm diagrams of BGn and the corresponding pore size distribution curve determined from the BJH desorption illustrated in its inset graph. In accordance with the IUPAC hysteresis loops classification, the hysteresis loop of prepared BGn is categorized as an H3 type. The hysteresis loop curve is given by non-rigid aggregates of plate-like particles or possibly the pore network consists of mesopores with split-like pores having adsorption high energy. The pore size distributions obtained by BJH measurement revealed the mesopores in the range of 1.2–6.9 nm peaked around 2 nm. The total pore volume of the prepared BGn was 0.17 cm^3/g and the specific surface area of the prepared BGn was also determined 121 m^2/g. SEM analysis of the cryogenically fractured surface of PP and PPB specimens is shown in Figure 2. It is observed that the PCL phase forms the spherulite-like phase with uniform dispersion throughout the PDLLA matrix. In PPB the distribution of BGn throughout the PDLLA/PCL matrix is also appropriate which is evidenced by EDS line scan profiles (Not shown) [8].

3.2. In vitro bioactivity studies

3.2.1. Morphological and phase characterization

The SEM images of PPB nanocomposites and PP blends incubated in SBF solution following for 0, 1, 2, and 4 weeks are illustrated in Figure 3.

The as-received SEM results (before incubation in SBF) obtained from PPB and PP specimens illustrated no significant difference in surface morphology where the PPB nanocomposites possess some smalls and narrow pores at the surface which could be resulted from air entrapping during the sample preparation. After 1 and 2 weeks of soaking, the amounts of porosities in PP specimens were increased which may be related to the biodegradation feature of PDLLA and PCL presented in PP blends. Moreover, the morphology of the surface in PP blends was roughed. The snowflake-like microstructure at the PP blend surface can be observed after 28 days of immersion. This could be due to the precipitation process of apatite layers at PP surfaces, however, the flake-like texture is not grown and is widely spread throughout the surface. In the case of nanocomposites, after one-week immersion in SBF, some pores owing to the degradation feature of PPB nanocomposites are shown. Besides, the formation of apatite precipitates after a one-week follow-up reveals that PPB nanocomposites are able to form more volume apatite at its surface in comparison with PP blends (white precipitates). The changes in nanocomposites surface morphology after 2 weeks of immersion are strongly obvious where spherical precipitates morphology on the surface are indicated. So that, 4 weeks follow-ups of SBF incubation revealed that the formed apatite crystals are widely grown and covered whole surfaces of PPB nanocomposites. That is clear because when a bioactive material is exposed to a physiologic solution, the calcium phosphate precipitates initiate to form on its surface. On the other hand, the addition of solid containing calcium phosphate compositions leads to supersaturate solution composition which is soluble into SBF, hence, local supersaturating changes toward apatite formation. Taking the case of amorphous bioactive glass, its alkaline cations make an increase in the pH of SBF. This increase in pH may lead to a notable decrease in HA solubility and consequently form abundant apatite nuclei. Besides

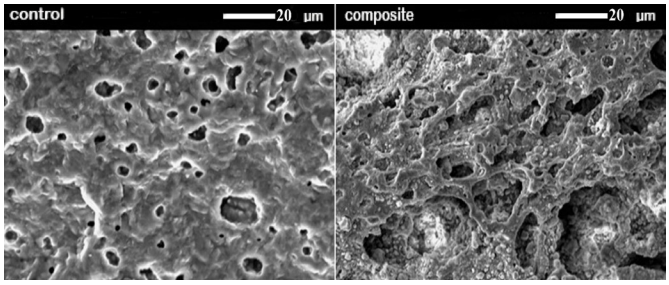

Fig. 6. SEM images of PPB and PP after immersion in PBS for 17- weeks follow up.

a pH change, the local solution composition can be modified by using a soluble material into SBF that can release large quantities of calcium and phosphate ions. This feature could be explained that how an implant containing Ca-P compositions could be directly bonded to living bone.

In Figures 4, the XRD patterns of PPB and PP specimens after immersion into SBF solution for different time intervals are shown. The peaks at 21 and 24 degrees may be related to the PDLLA matrix which is observed in whole patterns. The XRD patterns of PPB nanocomposites throughout the 1, 2 and 4 weeks follow up, display the some extra peaks which became more apparently by increasing in immersion times (Figure 4a). These peaks may be attributed to semi crystalline apatite calcium phosphate precipitates (JCPDS No: 24-0033). These low intensity and broadness of the bands can be understood since the XRD signal comes from a thin deposited layer. In contrast, in PP blends XRD patterns (Figure 4b), there are no peaks which confirm the presence of calcium phosphate precipitates on blends surfaces even after 4 weeks incubation in SBF.

3.2.2. Weight loss and pH assessments

Figure 5 displays the weight variations of PP and PPB specimens in SBF and PBS biological solutions during immersion times (4320 hours is equal to 180 days). The maximum weight loss changes in PBS solution are related to PP blends during whole evaluating times. In PBS, no weight gain of PP and PPB are identified and weight loss follows a constant trend up to 1440 hours. From 1440 to 2880 hours, the weight loss of whole specimens is increased and further increment in the following time up to 4320 hours presents a sharply rising trend for all of them. Overall, the PP and PPB specimens reveal 64% and 55 % weight loss at the end of immersion times in PBS solution, respectively. The weight loss evaluations of all specimens immersed into SBF show totally different behaviors. In the SBF, the weight loss percentages have firstly the falling trend. It means that by increasing the immersion time, weight gain occurs. These trends for PP blends and PPB nanocomposites continue up to 336 and 666 hours, respectively. After these sessions, the weight loss for both specimens shows increasing trends with a lower rate of up to 2880 hours and a higher rate of up to 4320 hours. In accordance with obtained results, the total weight loss of PP blends into SBF is higher in comparison with PPB nanocomposites. So, these values are about 45% and 36% for PP and PPB specimens at the end of the following time into SBF, respectively. Increasing in the weight loss rate after 1440 and 2880 hours may be ascribed to make porosities into the specimen's body. These findings occurred due to the degradation of the PDLLA phase into the structure of PP and PPB. These degradations may be caused to increase the exposing surface area of specimens with biological solutions and is therefore accelerated the weight loss rate.

This claim is evidenced by SEM images of specimens incubated in PBS (Figure 6). As is also found in Figure 5, the total weight loss of whole specimens in SBF *in-vitro* evaluations is lower than PBS one. This is due to the that the SBF is a calcium and phosphorus ions rich solution which causes to form calcium phosphate precipitates more probable on specimens surfaces immersed into SBF. This capability

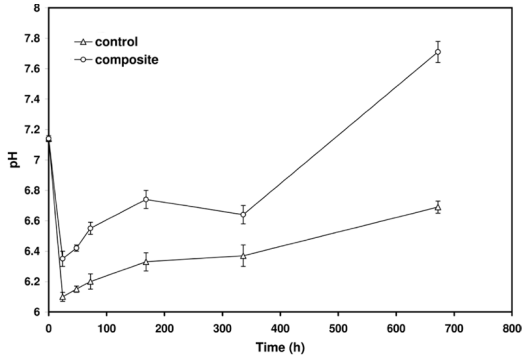

Fig. 7. PH variations of composites and control specimens as a function of immersion times into SBF.

for PPB nanocomposites is more likely. Since the PPB nanocomposites have calcium and phosphorus ions in their compositions, these ions could thermodynamically stimulate the calcium and phosphorus ions to precipitate formations. In addition, the calcium and phosphorus components in nanocomposites may provide proffered sites for apatite nucleation. These claims are evidenced by XRD patterns and SEM images of nanocomposites where the presences of apatite phases are obvious. This is while in PP XRD patterns are not realized any crystalline phases and also SEM images show the spares precipitates on specimen surfaces. However, the SEM images of PP obtained after 4 weeks show some narrow precipitates on its surface. It could be found that the initial weight gain for both PP and PPB specimens may be related to Ca-P precipitates on their surfaces. Polymeric phase degradations and calcium phosphate precipitate dissolutions cause lost weight of specimens while the precipitation phenomena cause gain weight of specimens. For PP and PPB specimens, weight loss commenced after 336 and 1440 hours, respectively. On the other hand, after these times, the degradation of polymeric and inorganic phases could be dominant rather than the Ca-P precipitates formation process. However, the weight loss for PPB nanocomposites is lower than PP blends. This may be due to inhibiting effect of Ca-P precipitates from the degradation process which is in high volumes on the surface of PPB nanocomposites. In addition, Ca-P precipitates could buffer the localized acidic pH resulting from acidic by-products of polymers degradation. The acidic circumstance could stimulate polymers' degradation. During *in-vitro* follow-up, the weight loss percentages of nanocomposites are about 9% lower than blends. The high amounts capabilities of Ca-P precipitates formation on nanocomposites surface into *in-vitro* solutions indicate the higher its bioactivity rather than blends specimens.

Figure 6, presents the SEM images of nanocomposites and blends after 17 weeks follow up in PBS media. As can be seen, the large voids (5 to 20 µm) could be related to the degradation process. In composites, one, the spheres-like phases are also observed. It seems that the precipitating and degradation processes simultaneously occur in PBS.

The pH variations of nanocomposites and blends specimens as a function of immersion times into SBF are presented in Figure 7. At first, the variation trends of both specimens show that the neutral pH of the solution moves initially toward acidic ranges as a function of immersion time where these decreases in pH of PP are more than of those nanocomposites. This may be owing to the release of acidic products resulting from PDLLA degradation as a major phase of both systems. While these materials were immersed into the SBF solution, hydrolysis of the PDLLA leads to generate lactic acid and the release of H^+ ions. The falling trend of pH variations for PP is initially sharp and after that have a rising trend due to Ca-P precipitates formations, however at the end of evaluating time is placed in acidic ranges. Whereas, the PPB specimens due to the introduction of BGn as an alkaline phase into its composition as well as Ca-P precipitates have a strong rising trend after the initial decrease. Moreover, the presence of BGn in the component of the nanocomposites

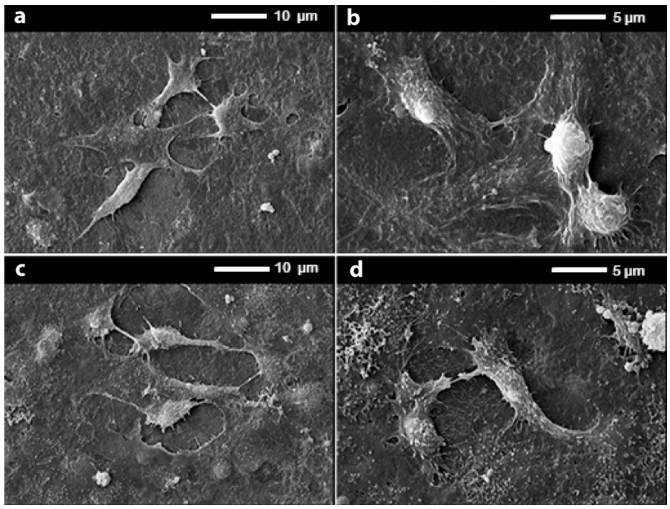

Fig. 8. Morphology of MG-63 cell line adhesion on (a and b) PP as a control group and (c and d) PPB as composite groups at different magnifications after 1 day of culture.

may be acted as crystal nuclei which could promote the process of apatite crystals forming on the surface of the material. The formation of new apatite crystal also avoids accessing SBF solution to nanocomposites interface, leading to slow hydrolysis of PDLLA phase in nanocomposites. This is caused to reach pH 7.7 at the end of the following time.

3.2.3. Evaluation of Adhesion and Morphology of human osteoblast cell line (MG-63)

Remodeling of bone is assumed that the progenitor cells whether transferred or formed at damaged bone sites able to remodel or reconstruct the damaged or lost bone tissues [25]. The cell supplier for bone tissue engineering according to differentiation capabilities were categorized into: stem cells, bone marrows, and osteoblast cells. Regarding the formation of extracellular matrix (ECM), the osteoblast cells are more effective [26]. Figure 8 compares the morphology of osteoblast cells attached to PP (figure 8(a, b)) and PPB (figure 8(c, d)) with different magnifications after 1 day of culture. As can be found, the cytoplasmic membrane of MG-63 cells is attached and spread in spindle-like morphology on the surface of both PP and PPB after 1 day of incubation. Also, cytoplasmic membrane creates filopodial structures with polyhedral morphology. It is also seen that migrating cells form ECM which may be displayed the good cell migration and osteoconduction characteristics of implants. Level of cell attachments and proliferation in order to evaluate the biocompatibility included: cell adhesion or attachment, filopodia extension, cross-linking, and spreading levels. The obtained results reveal that our implants in terms of biocompatibility are laid on the forth level.

Generally, the principle of MTT assay is based on the conversion of MTT into formazan crystals which reflects the mitochondrial activity. For most cells, the mitochondrial activity is constant and thus, the increase or decrease in viable cells population possesses a linear trend with mitochondrial activity. Since the total mitochondrial activity of the cell population depends on the number of viable cells, this assay can be applied to *in-vitro* solutions that contain cell lines or initial patient cells in order to evaluate the biomaterials cytotoxicity effects [27]. In this regard, the conversion of the tetrazolium salts MTT into formazan crystals by cell mitochondrial activities can be assumed as a measuring criterion. Thus, any increase or decrease of viable cells number can be calculated using measuring of formazan concentration by optical density (OD). The MTT assay results illustrate that both PP and PPB specimens follow the increasing trends of cell formazan population as a function of culturing times (Figure 9a). However, the number of viable cells on PP during 1-day and 3-day of culturing times is higher in comparison with PPB, and increasing in culturing times up to 14 days led to the most viability of cells is belonged to PPB, there are no statistically significant differences between the obtained results (P>0.05). The MTT assay results demonstrate the desirable cell proliferation in the vicinity of whole specimens.

Figure 9b shows the ALP activity of PP and PPB specimens. The ALP is considered to be an initial marker of osteoblast differentiation and suggests bone formation activity. As demonstrated in Figure 9b, after 3 days, the cell activity on PP is more than that on PPB, although there is no statistically significant difference. By increasing in culturing times up to 21 days, the secretion of ALP enzymes on PPB implants is remarkably increased in comparison with PP. On the other hand, after 1, 2, and 3 weeks, the osteoblast cell grows and the mineralization capability of PPB has been increased in comparison with PP. Generally, in order to obtain results of MTT assay and ALP studies, it can be concluded that the introduction of BG nanoparticles in PPB implants is able to stimulate the proliferation and activity of osteoblast cells as well as play an effective role in bone formation especially after high incubation times in culture medium.

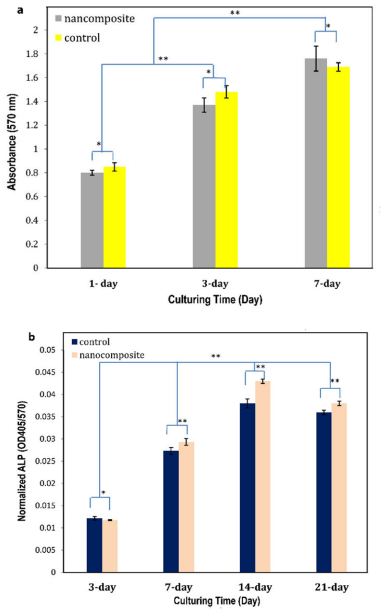

Fig. 9. (a) MTT assay of PPB nanocompos-ites and PP blends as control as function of different culture times. (b) ALP activity of PPB and PP after 3 day, 1 week, 2 week and 3 weeks of culturing times (*P>0.05 and **P<0.05).

4. Conclusions

From the results of this study, the following conclusions can be pointed out:

- The studies of morphology and phase variations throughout the SBF and PBS solutions confirm the high capabilities of PPB implants rather than PP ones on Ca-P precipitates formation due to the presence of bioglass.
- The degradation rate, weight loss changes, and pH variations of PP implants during different times of *in-vitro* evaluations are more considerable rather than PPB ones.
- The MTT assay reveals no toxicity for both implants, and cell proliferation as well as cell attachment results determine that the cells can easily proliferate and attach with filopodial extension morphology on PPB surfaces compared to PP blends.
- The ALP results obtained from 3 weeks of follow-ups approve the more activity of osteoblast cells on bone formation throughout the PPB implants in comparison with PP ones.

Acknowledgment

The authors wish to acknowledge Esfarayen University of Technology (EUT) and Materials and Energy Research center (MERC) for the all supports throughout this work.

Funding

The research leading to these results received funding from the ministry of industry mine and trade of the Islamic Republic of Iran under Grant Agreement No. 93/41/5659. Partial financial support was also received from Esfarayen University of Technology (EUT).

Conflict of Interest

The authors declare that there is no conflict of interest.

REFERENCES

[1] T. Zantop, A. Weimann, R. Schmidtko, M. Herbort, M.J. Raschke, W. Petersen, Graft laceration and pullout strength of soft-tissue anterior cruciate ligament reconstruction: in vitro study comparing titanium, poly-d, l-lactide, and poly-d, l-lactide–tricalcium phosphate screws, Arthroscopy: The Journal of Arthroscopic & Related Surgery 22(11) (2006) 1204-1210.

[2] R. Papalia, S. Vasta, S. D'Adamio, A. Giacalone, N. Maffulli, V. Denaro, Metallic or bioabsorbable interference screw for graft fixation in anterior cruciate ligament (ACL) reconstruction?, British medical bulletin 109(1) (2014) 19-29.

[3] P. Debieux, C.E. Franciozi, M. Lenza, M.J. Tamaoki, R.A. Magnussen, F. Faloppa, J.C. Belloti, Bioabsorbable versus metallic interference screws for graft fixation in anterior cruciate ligament reconstruction, Cochrane Database of Systematic Reviews (7) (2016).

[4] A.-S. Moisala, T. Järvelä, A. Paakkala, T. Paakkala, P. Kannus, M. Järvinen, Comparison of the bioabsorbable and metal screw fixation after ACL reconstruction with a hamstring autograft in MRI and clinical outcome: a prospective randomized study, Knee Surgery, Sports Traumatology, Arthroscopy 16 (2008) 1080-1086.

[5] C. Kaeding, J. Farr, T. Kavanaugh, A. Pedroza, A prospective randomized comparison of bioabsorbable and titanium anterior cruciate ligament interference screws, Arthroscopy: The Journal of Arthroscopic & Related Surgery 21(2) (2005) 147-151.

[6] F.D. Bach, R.Y. Carlier, J.B. Elis, D.M. Mompoint, A. Feydy, O. Judet, P. Beaufils, C. Vallée, Anterior cruciate ligament reconstruction with bioabsorbable polyglycolic acid interference screws: MR imaging follow-up, Radiology 225(2) (2002) 541-550.

[7] J.C. Middleton, A.J. Tipton, Synthetic biodegradable polymers as orthopedic devices, Biomaterials 21(23) (2000) 2335-2346.

[8] J. Esmaeilzadeh, S. Hesaraki, S.M.-M. Hadavi, M.H. Ebrahimzadeh, M. Esfandeh, Poly (d/l) lactide/polycaprolactone/bioactive glasss nanocomposites materials for anterior cruciate ligament reconstruction screws: The effect of glass surface functionalization on mechanical properties and cell behaviors, Materials Science and Engineering: C 77 (2017) 978-989.

[9] J. Esmaeilzadeh, S. Hesaraki, M.H. Ebrahimzadeh, G.H. Asghari, A.R. Kachooei, Creep behavior of biodegradable triple-component nanocomposites based on PLA/PCL/bioactive glass for ACL interference screws, Archives of Bone and Joint Surgery 7(6) (2019) 531.

[10] T. Niemelä, M. Kellomäki, Bioactive glass and biodegradable polymer composites, Bioactive Glasses, Elsevier2011, pp. 227-245.

[11] V.V. Meretoja, T. Tirri, M. Malin, J.V. Seppälä, T.O. Närhi, Ectopic bone formation in and soft-tissue response to P (CL/DLLA)/bioactive glass composite scaffolds, Clinical oral implants research 25(2) (2014) 159-164.

[12] H.O. Mayr, R. Hube, A. Bernstein, A.B. Seibt, W. Hein, R. von Eisenhart-Rothe, Beta-tricalcium phosphate plugs for press-fit fixation in ACL reconstruction—a mechanical analysis in bovine bone, The Knee 14(3) (2007) 239-244.

[13] Y. Arama, L.J. Salmon, K. Sri-Ram, J. Linklater, J.P. Roe, L.A. Pinczewski, Bioabsorbable versus titanium screws in anterior cruciate ligament reconstruction using hamstring autograft: a prospective, blinded, randomized controlled trial with 5-year follow-up, The American journal of sports medicine 43(8) (2015) 1893-1901.

[14] M.C. Park, J.E. Tibone, False magnetic resonance imaging persistence of a biodegradable anterior cruciate ligament interference screw with chronic inflammation after 4 years in vivo, Arthroscopy: The Journal of Arthroscopic & Related Surgery 22(8) (2006) 911. e1-911. e4.

[15] W.H. Warden, D. Chooljian, D.W. Jackson, Ten-year magnetic resonance imaging follow-up of bioabsorbable poly-L-lactic acid interference screws after anterior cruciate ligament reconstruction, Arthroscopy: The Journal of Arthroscopic & Related Surgery 24(3) (2008) 370. e1-370. e3.

[16] G. Schmidmaier, K. Baehr, S. Mohr, M. Kretschmar, S. Beck, B. Wildemann, Biodegradable polylactide membranes for bone defect coverage: biocompatibility testing, radiological and histological evaluation in a sheep model, Clinical oral implants research 17(4) (2006) 439-444.

[17] R. Kontio, P. Ruuttila, L. Lindroos, R. Suuronen, A. Salo, C. Lindqvist, I. Virtanen, Y.T. Konttinen, Biodegradable polydioxanone and poly (l/d) lactide implants: an experimental study on peri-implant tissue response, International journal of oral and maxillofacial surgery 34(7) (2005) 766-776.

[18] E. Waris, N. Ashammakhi, M. Lehtimäki, R.-M. Tulamo, M. Kellomäki, P. Törmälä, Y.T. Konttinen, The use of biodegradable scaffold as an alternative to silicone implant arthroplasty for small joint reconstruction: an experimental study in minipigs, Biomaterials 29(6) (2008) 683-691.

[19] M. Barbeck, T. Serra, P. Booms, S. Stojanovic, S. Najman, E. Engel, R. Sader, C.J. Kirkpatrick, M. Navarro, S. Ghanaati, Analysis of the in vitro degradation and the in vivo tissue response to bi-layered 3D-printed scaffolds combining PLA and biphasic PLA/bioglass components–Guidance of the inflammatory response as basis for osteochondral regeneration, Bioactive materials 2(4) (2017) 208-223.

[20] Z. Guo, D. Bo, Y. He, X. Luo, H. Li, Degradation properties of chitosan microspheres/poly (L-lactic acid) composite in vitro and in vivo, Carbohydrate polymers 193 (2018) 1-8.

[21] T.T. Nguyen, T. Hoang, A.S. Ho, S.H. Nguyen, T.T.T. Nguyen, T.N. Pham, T.P. Nguyen, T.L.H. Nguyen, M.T.D. Thi, In vitro and in vivo tests of PLA/d-HAp nanocomposite, Advances in Natural Sciences: Nanoscience and Nanotechnology 8(4) (2017) 045013.

[22] C.B. Danoux, D. Barbieri, H. Yuan, J.D. de Bruijn, C.A. van Blitterswijk, P. Habibovic, In vitro and in vivo bioactivity assessment of a polylactic acid/hydroxyapatite composite for bone regeneration, Biomatter 4(1) (2014) e27664.

[23] J. Esmaeilzadeh, S. Hesaraki, S.M.-M. Hadavi, M. Esfandeh, M.H. Ebrahimzadeh, Microstructure and mechanical properties of biodegradable poly (D/L) lactic acid/polycaprolactone blends processed from the solvent-evaporation technique, Materials Science and Engineering: C 71 (2017) 807-819.

[24] H.A. Krebs, Chemical composition of blood plasma and serum, Annual review of biochemistry 19(1) (1950) 409-430.

[25] W. Zhang, X.F. Walboomers, T.H. van Kuppevelt, W.F. Daamen, Z. Bian, J.A. Jansen, The performance of human dental pulp stem cells on different three-dimensional scaffold materials, Biomaterials 27(33) (2006) 5658-5668.

[26] Z.-Y. Zhang, S.-H. Teoh, M.S. Chong, E.S. Lee, L.-G. Tan, C.N. Mattar, N.M. Fisk, M. Choolani, J. Chan, Neo-vascularization and bone formation mediated by fetal mesenchymal stem cell tissue-engineered bone grafts in critical-size femoral defects, Biomaterials 31(4) (2010) 608-620.

[27] J. Van Meerloo, G.J. Kaspers, J. Cloos, Cell sensitivity assays: the MTT assay, Cancer cell culture: methods and protocols (2011) 237-245.